Excitonic order at strong coupling: Pseudospin, doping, and ferromagnetism

Leon Balents
Physics Department, University of California, Santa Barbara, California 93106
(Received 6 March 2000)

A tight-binding model is introduced to describe the strong interaction limit of excitonic ordering. At stoichiometry, the model reduces in the strong-coupling limit to a pseudospin model with approximate U(4) symmetry. Excitonic order appears in the pseudospin model as in-plane pseudomagnetism. The U(4) symmetry unifies all possible singlet and triplet order parameters describing such states. Superexchange, Hunds-rule coupling, and other perturbations act as anisotropies splitting the U(4) manifold, ultimately stabilizing a paramagnetic triplet state. The tendency to ferromagnetism with doping (observed experimentally in the hexaborides) is explained as a spin-flip transition to a different orientation of the U(4) order parameter. The physical mechanism favoring such a reorientation is the enhanced coherence (and hence lower kinetic energy) of the doped electrons in a ferromagnetic background relative to the paramagnet. A discussion of the physical meaning of various excitonic states and their experimental consequences is also provided.

I. INTRODUCTION

The unexpected discovery of high-T_c itinerant ferromagnetism in doped hexaborides[1] has reignited interest in the problem of excitonic ordering near the semiconductor-metal transition.[2,3] Excitonically ordered states are characterized by an off-diagonal order parameter describing pairing between conduction electrons and valence holes. Early theoretical work by Volkov *et al.*[4] anticipated the emergence of ferromagnetism on doping such an excitonic state. These authors considered the limit of nearly nested overlapping conduction and valence bands with *weak* repulsive electron-electron interactions. In this limit, the problem can be approximately cast into a form nearly identical to BCS theory, and studied using the techniques of mean-field theory. Although this work (and some subsequent recent studies[5]) suffered from the important physical mistake of neglecting the instability to phase separation, ferromagnetism nevertheless remains a generic feature in a corrected treatment.[6,7]

While the appearance of ferromagnetism in the weak-coupling limit is encouraging, it is far from a conclusive and complete theoretical explanation for the experiments. First, Coulomb interactions in the hexaborides are not particularly weak, and most likely are comparable to the Fermi energy and band overlap. Second, the above explanation appears to hinge on the first-order nature of the excitonic to normal (E-N) transition in the BCS limit. While this feature, mathematically analogous to the first-order transition to the normal state due to pair breaking by an external Zeeman field in a superconductor,[8,9] is present in the nested mean-field limit, there do not appear to be any general theoretical grounds mandating this behavior more generally. Moreover, the universality of the experimental results, now observed in a large number of different compounds ($Ca_{1-x}La_xB_6$, BaB_6, $Ca_{1-x}Ce_xB_6$, SrB_6, etc.),[10] argues for the robustness of the phenomenon.

To determine whether excitonic ferromagnetism is indeed more general than its weak-coupling theoretical basis, here we consider the completely opposite *strong-coupling* regime. This is not expected to be directly applicable to the hexaborides, as these materials are most likely best described by an intermediate-coupling model. Nevertheless, many useful insights are gained from this complementary limit. As usual, the principal assumption of the strong-coupling limit is the dominance of potential energy over kinetic energy. This is achieved concretely using a tight-binding model [see Eqs. (4)–(7), in Sec. II], in which the conduction and valence bands of the conventional continuum theories are replaced by localized a and b orbitals, respectively. The analog of the band gap in the continuum model is the level splitting $E_G = E_a - E_b > 0$. The order parameter characterizing excitonic ordering is then a matrix in spin space,

$$\Delta_{\alpha\beta} = a_\alpha^\dagger b_\beta, \tag{1}$$

where $a_\alpha^\dagger$ creates an electron with spin $\alpha = \uparrow, \downarrow$ in the a orbital, and b_β annihilates an electron with spin β in the b orbital. Excitonically ordered states thus have some partial occupation of the nominally excited a states, as a result of Coulombic repulsion. In general, $\Delta_{\alpha\beta}$ is a proper order parameter (i.e., one which characterizes a spontaneously broken symmetry) if the a and b orbitals have different symmetries. In this paper, we consider a ''minimal model'' with this property, comprised of one a and one b orbital per unit cell—see Fig. 1. This mimics the situation in the hexaborides, for which the conduction and valence states also transform as different representations of the cubic point group.[11] Because of complications arising from orbital degeneracy, however, the appropriate representations for the hexaborides are three dimensional rather than scalar. We defer the possible complications arising from these additional degrees of freedom to a future investigation.

As for the more familiar Hubbard model (see, e.g. Ref. 12), the problem simplifies somewhat in the strong-coupling limit. Considering first the undoped system (half-filled, or two electrons per unit cell), we obtain a quantum pseudospin model [Eqs. (8)–(12), Sec. III]. Within this model, the excitonic insulator (EI) appears as an intermediate state separating not a metal and a semiconductor but a *Mott insulator* and a semiconductor (or band insulator). In some respects, the

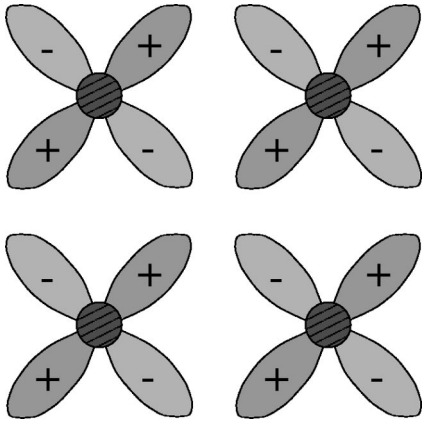

FIG. 1. Imaginative illustration of a model for which the tight-binding description employed phenomenologically here directly applies. Red circles and blue plus green crosses represent s and d_{xy} orbitals, respectively.

behavior is argued to be quite similar to that of a quantum spin-1/2 XXZ antiferromagnet in a magnetic field, with excitonic ordering analogous to XY antiferromagnetism. The ''spins'' of the model, however, can take on *five* distinct states per site: one singlet state with both electrons in the lower-energy b orbital, and four different spin states with one a electron and one b electron. This is in contrast to the two states of a single spin-1/2 particle.

In the strong-coupling limit, this large Hilbert space is ''unified'' by several approximate symmetries valid at different energy scales. At the largest energy scales this is an enormous SU(4) group, corresponding to arbitrary complex rotations of the four components of $\Delta_{\alpha\beta}$. The approximate SU(4) symmetry fully unifies all possible excitonic states, including singlet, triplet, and singlet-triplet coexistences. These are described by the general decomposition

$$\Delta = \frac{1}{2}(\Delta_s \mathcal{I} + \vec{\Delta}_t \cdot \vec{\sigma}^*), \tag{2}$$

where Δ_s and $\vec{\Delta}_t$ are the singlet and triplet order parameters, and $\mathcal{I}$ and $\vec{\sigma}$ are the 2×2 unit and Pauli matrices in spin space, respectively. A system with approximate SU(4) invariance contains the germ of ferromagnetism, since several possible excitonic states (those with nonzero $\mathrm{Re}\,\Delta_s \vec{\Delta}_t^*$ and/or $\mathrm{Im}\,\vec{\Delta}_t \wedge \vec{\Delta}_t^*$) give rise to net exchange fields, and hence a magnetic moment. SU(4) symmetry implies that these states are low in energy. At intermediate energies the SU(4) symmetry reduces to an $\mathrm{SU}(2)\times\mathrm{SU}(2)$ invariance, which reflects separate spin rotations of the a and b electrons. The latter is a symmetry of the conventional continuum models of EI's, and transforms the order parameter in a ''chiral'' manner: $\Delta \to U_L^\dagger \Delta U_R$, where U_L and U_R are SU(2) matrices. Finally, further weak interactions reduce this to a simple $\mathrm{SU}(2)\times Z_2$ symmetry at the (very) lowest energies.

These symmetry considerations underly the simple physical mechanism for ferromagnetism elucidated here.[13] The dominant tendency imposed by Coulomb interactions is to excitonic ordering. With approximate SU(4) symmetry, however, the ''orientation'' (form of $\Delta_{\alpha\beta}$) of the order parameter is nearly free, and fixed only by weak ''anisotropy'' terms. In the undoped material, these anisotropies favor a simple paramagnetic triplet state. Doping introduces additional exchange energy contributions that modify the anisotropy, causing $\Delta_{\alpha\beta}$ to ''flip'' into a different orientation with a ferromagnetic moment. In the present model, the excitonic order in the ferromagnet is of non-collinear triplet type, in which

$$\Delta_s = 0, \quad \vec{\Delta}_t \wedge \vec{\Delta}_t^* \neq 0. \tag{3}$$

As shown in Sec. V, in addition to ferromagnetic magnetization, this state has additional spatially-varying local static moments and spin currents transverse to the axis of net magnetization. The transition to this state from the paramagnet is generally first order, and therefore coincides with a jump in the electronic density. Since experiments are performed at fixed charge density (dictated by the concentration of dopant ions), the intermediate ''forbidden'' range of dopings can be accommodated only by phase separation. With long-range Coulomb interactions included, macroscopic phase separation is impossible, and charge domain formation is expected, as already pointed out in Refs. 6 and 7.

The *detailed* demonstration of this behavior with doping is nontrivial. As for many other strongly correlated systems, the problem of doping is much more difficult than that of the stoichiometric Mott insulator. Indeed, as the EI state lies intermediate between band and Mott insulators, doping the EI is a sort of interpolation between doping a conventional band insulator and doping an antiferromagnetic insulator. The latter problem is of course at the crux of the physics of high-temperature superconductivity, so that perhaps the experimental and theoretical insights gained in the hexaborides will be more generally helpful. At any rate, doping the EI can be shown by very simple arguments to favor ferromagnetism in strong coupling. Essentially, the physics of this behavior is similar to the ''Nagaoka effect''[14] in a doped antiferromagnet—ferromagnetic alignment of the excitonic order parameters allows for more coherent propagation of the doped electrons, and hence a lowering of their kinetic energy. This mechanism is actually *stronger* in the EI than in the antiferromagnet, because of the global *coherence* of the excitonic condensate, and the near degeneracy [due to approximate SU(4) symmetry] of ferromagnetic and paramagnetic states. To provide a concrete demonstration of these ideas, the strong-coupling zero-temperature phase diagram of the model is calculated in this paper using a ''free Fermi gas'' approximation. This approximation captures the most important *single quasiparticle* physics of electronic propagation in an excitonically ordered background, but neglects interactions between these quasiparticles. For simplicity, we also assume a *fixed amplitude* $\mathrm{Tr}\,\Delta^\dagger\Delta = \Delta_0^2/2$ of the excitonic order parameter. The latter assumption is valid for weak doping, $x \ll 1$, in which the *orientation* of the ordering is of paramount importance. Putting together the results of this calculation and the stoichiometric behavior, we arrive at the partial phase diagram in Fig. 2. This is in agreement with the general expectations stated above. It should be stressed, however, that this analysis of doping is far from exhaustive. More detailed investigations of both the weak- and strong-coupling limits are currently underway.[15]

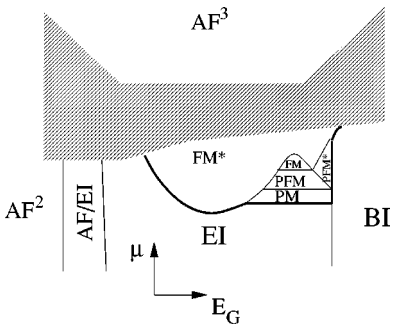

FIG. 2. Partial phase diagram of the strong-coupling model as a function of E_G (half the bare splitting between *a* and *b* orbitals), and μ, the chemical potential. The shaded region is not analyzed in this paper. Thick lines indicate the boundary between the undoped region below (with two electrons per unit cell) and the doped region above (with more than two electrons per unit cell). The AF^2 and AF^3 phases are antiferromagnetic Mott insulators with two and three electrons per unit cell, respectively. The BI state is the band insulator. Intermediate between the BI and AF^2 phases are the excitonic insulator (EI) and an insulator with coexisting excitonic and Neél order (EI/AF). The FM, FM*, PFM, and PFM* phases are all ferromagnetic metals (see Table I for the differences between these states), while PM indicates a paramagnetic metallic phase. All the metallic states above exhibit excitonic order.

The remainder of the paper is structured as follows. In Sec. II, we present a detailed exposition of the (simplest) tight-binding model capable of describing excitonically ordered states, and consider the limit of infinite interaction strength. The bulk of the paper is contained in Sec. III, where the model is analyzed for large but finite interactions, focusing on the stoichiometric situation with two valence electrons per unit cell. For this electron density the model is insulating, but can sustain excitonic and other types of ordering. The properties of the model with doping are discussed in Sec. IV. We conclude in Sec. V with a clarifying discussion delineating the physical properties of various possible excitonic insulators, and the relation of the results of this paper to the hexaborides.

II. TIGHT-BINDING MODEL

A. ''On-site'' terms

We consider a minimal model capable of exhibiting excitonic order, which contains two orbitals per unit cell, so as to give rise to two bands in a noninteracting limit (the actual situation in the hexaborides is more complex, with orbital degeneracy leading to multiple electron and hole pockets). A strong-coupling limit is obtained by first considering only *local* interactions within a unit cell,

$$H_0=\sum_i E_G(a_i^\dagger a_i-b_i^\dagger b_i)-\mu(a_i^\dagger a_i+b_i^\dagger b_i) + U(a_{i\uparrow}^\dagger a_{i\uparrow}a_{i\downarrow}^\dagger a_{i\downarrow}+b_{i\uparrow}^\dagger b_{i\uparrow}b_{i\downarrow}^\dagger b_{i\downarrow})+Va_i^\dagger a_i b_i^\dagger b_i, \quad (4)$$

where *a* and *b* are electron annihilation operators for the ''conduction'' and ''valence'' states, respectively, obeying $\{a_{i\alpha},a_{j\beta}^\dagger\}=\{b_{i\alpha},b_{j\beta}^\dagger\}=\delta_{ij}\delta_{\alpha\beta}$. Here and throughout the paper, we use Latin indices $i,j,\ldots$ to denote the lattice site, and Greek indices $\alpha,\beta,\ldots=\uparrow,\downarrow$ to denote the spin state. Labels will be suppressed and implicit wherever clarity allows. The parameters E_G,μ,U,V describe the ''band gap'' (orbital energy difference), chemical potential, on-site ''Hubbard'' repulsion, and nearest-neighbor repulsion, respectively, within the unit cell.

A crucial feature of H_0 is the absence of direct hopping between the *a* and *b* orbitals within the unit cell. For excitonic ordering to be well defined, it is necessary at a minimum that the *a* and *b* states be distinguished by a discrete symmetry operation, e.g., parity. When this is the case, direct hopping between these orbitals is prohibited. It may be helpful to imagine an artificial situation in which the *a* and *b* orbitals represent *s* and d_{xy} orbitals on a single site of a square lattice (see Fig. 1).

In this situation, *a* and *b* orbitals are orthogonal both on the same site and on nearest-neighbor sites. An overlap *is* possible, though for next-nearest-neighbor pairs, i.e., on a diagonal. In general, an exchange interaction *is* allowed by symmetry, and takes the form

$$H_1=-J_H\sum_i \vec{S}_{ia}\cdot\vec{S}_{ib}, \quad (5)$$

where $\vec{S}_{ia}=\frac{1}{2}a_i^\dagger\vec{\sigma}a_i$ and $\vec{S}_{ib}=\frac{1}{2}b_i^\dagger\vec{\sigma}b_i$. Here and in the following, the Pauli matrices $\vec{\sigma}$ act in the spin space. On physical grounds, a ferromagnetic exchange ($J_H>0$) is most appropriate due to Hund's rule effects for orthogonal orbitals. For pedagogical purposes, we may wish to consider instead the opposite antiferromagnetic sign for this exchange. From the discussion in Sec. I, it is clear that an essential ingredient for excitonic ferromagnetism is the near degeneracy of singlet and triplet states. To build this into the strong-coupling model thus requires small J_H. For the majority of the paper, therefore, we will neglect J_H or treat it as a small perturbation.

B. Infinite interaction limit

The analysis of the strong-coupling limit begins by first considering the on-site Hamiltonian $H_{\rm site}=H_0+H_1$ in the absence of electron hopping between adjacent unit cells. This may be thought of as the analog of the $U=\infty$ analysis of an ordinary Hubbard model. In this case, the occupation of each orbital is a good quantum number, and the states can be straightforwardly enumerated. Assuming $E_G>V>0$, and at first also $J_{ab}=0$, one obtains the phase diagram shown in Fig. 3.

For the present study, we are particularly interested in densities near two electrons per unit cell. Note that the doping behavior (i.e. on increasing μ) in this regime depends crucially on the relative strength of E_G and U. In particular, for $2E_G>U-V$, the preferred charge $Q=2e$ state is one with both electrons in the lower orbital, corresponding to the band insulator. For $U-V>2E_G$, by contrast, the two-electron ground state has one electron in each orbital, and hence a net spin on each site. This is the ultrastrong coupling (i.e., local) version of a Mott insulator. Note that *neither* of these two states exhibits an *excitonic* order. This can be seen by directly computing $\langle a^\dagger b\rangle=0$ in either state. In fact, the

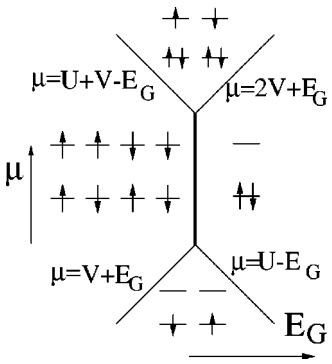

FIG. 3. Strong-coupling (ultralocal) phase diagram in the E_G-μ plane, neglecting exchange and all intercell hopping and interactions. Regions with zero and four electrons per unit cell are not shown. In each phase, the lowest-energy states are pictured, with an *a* orbital above and a *b* orbital below.

operators $a^\dagger b$ and $b^\dagger a$ act to transform the two phases into one another, i.e., move an electron from the lower to upper orbital, or vice versa.

C. Hopping terms

To investigate further, we must introduce hopping between adjacent cells. We will principally consider the simplest such term

$$H' = \sum_{\langle ij \rangle} t(a_i^\dagger a_j + b_i^\dagger b_j + \text{H.c.}), \tag{6}$$

where $\langle ij \rangle$ indicates that the sum is over nearest-neighbor pairs of sites. Different hopping integrals t_a and t_b between the two orbitals can also be easily included, but do not change the results significantly, so we will keep $t_a = t_b = t$ for simplicity [see, however, the discussion of particle-hole symmetry in Sec. V surrounding Eqs. (51)–(55)]. In general, there are also hopping processes connecting *a* and *b* orbitals. Due to the symmetry of the orbitals in Fig. 1, these occur only for next-nearest neighbors,

$$H'' = \sum_{\langle\langle ij \rangle\rangle} t_{ab}\ \text{sgn}[(x_i - x_j)(y_i - y_j)](a_i^\dagger b_j + \text{H.c.}), \tag{7}$$

where the double angular brackets denote a sum over next nearest neighbors *i* and *j*. Note that the hopping matrix elements in Eq. (7) are real, and vary in sign. The sign variations reflect the symmetry differences (under rotations) between the *s* and *d* orbitals. The reality of the coefficients is a matter of convention, which we fix by choosing the orbital wave functions to be real. We will assume, as appropriate in this example, that $t_{ab} \ll t$, so that H'' is small, and can therefore be treated perturbatively.

It is sometimes an important perturbation, because it reduces the symmetry of the Hamiltonian. In particular, all of the terms in $H_0 + H_1 + H'$ conserve the number of *a* and *b* particles separately. Neglecting the *a*-*b* hopping, therefore, the model has $\text{SU}(2) \times \text{U}(1) \times \text{U}(1)$ continuous symmetries, corresponding to conservation of spin, and *a* and *b* charges. The perturbation H'' reduces the continuous symmetries of the model down to $\text{SU}(2) \times \text{U}(1)$ corresponding to spin and total charge, which are required by the physics of the system. Equation (7) actually still respects a number of discrete symmetries, such as $b \to -b$ simultaneously with a $\pi/2$ rotation. These symmetries, which in fact comprise the point-group operations of the square lattice, can be viewed as a residual discrete subgroup of the original U(1) present in the absence of H''. We will see in Sec. III that this gives rise to an Ising symmetry under which the excitonic order parameters transform.

III. EFFECTIVE THEORY FOR THE UNDOPED SYSTEM

In the central region of Fig. 2, e.g., for $(U+V)/2 < \mu < (U+3V)/2$, all sites are doubly occupied in the strong coupling limit. Nevertheless, for $2E_G \leqslant U - V$, the low-energy states are highly degenerate. Well to the left of the thick vertical line, each *a* and *b* orbital is singly occupied, so that there are effectively two spin-1/2 degrees of freedom in each unit cell. In the infinite coupling limit these are completely free, but they will interact due to virtual hopping processes when H' (and H'') is included. Far to the right of the vertical line, the unique low-energy state consists of a doubly occupied *b* orbital in each unit cell, and hopping is unimportant. As the vertical line is approached from either side, virtual hopping processes can induce interactions involving all *five* low-energy states.

A. Bosonic *t*-*J* model

In this subsection, we develop an effective model for the interesting region near the vertical line. In this region, it is necessary and sufficient to truncate the Hilbert space to just the five low-energy states in each unit cell (although higher-energy states must be kept in virtual processes). The physics is amusingly similar to a sort of generalized bosonic *t*-*J* model. On the left-hand side of the thick vertical line, each unit cell is occupied by two spins. At second order in H', these interact via effective exchange interactions,

$$H^s_{\text{eff}} = \sum_{\langle ij \rangle} J(\vec{S}_{ia} \cdot \vec{S}_{ja} + \vec{S}_{ib} \cdot \vec{S}_{jb}) - \sum_i J_H \vec{S}_{ia} \cdot \vec{S}_{ib}, \tag{8}$$

where $J = t^2/(V + 2E_G)$. This exchange constant may be obtained by perturbatively computing the energy difference between singlet and triplet states on a bond to second order in the hoppings, and neglecting the deviation from the vertical line (i.e., setting $U = 2E_G + V$) in the denominators. The latter approximation is valid provided $|U - V - 2E_G| \ll V$. Well to the left of the vertical line (in particular when $U - V - 2E_G \gg t$), no doubly occupied *b* states are present, and Eq. (8) is a complete model. It describes two ferromagnetically bulk coupled Heisenberg spin-1/2 antiferromagnets. On a hypercubic lattice (square or cubic in two or three dimensions, respectively), one expects long-range antiferromagnetic order of spins on the same orbital sublattice, with *a* and *b* spins aligned parallel at each site.

As the vertical line is approached, the energy cost of a doubly occupied *b* orbital is reduced toward zero, and they must be introduced into the lattice. Unit cells with both electrons in the *b* orbital act as ''holes,'' having no associated local moment. Unlike the usual *t*-*J* model holes, they are, however, bosonic and neutral (relative to the magnetic state,

they represent the removal of an a electron and replacement with a b electron). Hole hopping occurs at second order in t,

$$H^h_{\rm eff} = -\mu_h \sum_i h_i^\dagger h_i + t_h \sum_{\langle ij\rangle} (h_i^\dagger h_j + h_j^\dagger h_i)\mathcal{P}_{ij} + \sum_{\langle ij\rangle} V_{hh} h_i^\dagger h_i h_j^\dagger h_j , \tag{9}$$

where $\mu_h = 2E_G - U + V + t^2/(2V) - t^2/[2(2E_G+V)]$ is the hole ''chemical potential,'' $t_h = t^2/(2V)$, $V_{hh} = t^2/V - \frac{1}{2}t^2/(2E_G+V)$, and $\mathcal{P}_{ij} = (\frac{3}{2} + 2\vec{S}_{ia}\cdot\vec{S}_{ja})(\frac{3}{2} + 2\vec{S}_{ib}\cdot\vec{S}_{jb})$ is the operator which interchanges the spin states at sites i and j. As in a conventional doped antiferromagnet, the presence of the $\mathcal{P}_{ij}$ operator in the hopping term leads to difficulties of hole motion in an antiferromagnetic spin background. Naive successive hopping of a single hole in an antiferromagnetic state results in a generalization of the well-known ''string'' of misaligned spins in its wake.

Introducing the a-b hopping term [Eq. (7)] affects the system in several ways. There are renormalizations of the coupling constants in Eqs. (9) and (8), of order t_{ab}^2/V, $t_{ab}^2/(V+4E_G)$. Since, by assumption, $t_{ab} \ll t$, these are negligible. New exchange couplings are also generated between next-nearest-neighbor a and b spins, which were not previously present. Because they are small, unfrustrating, and break no additional symmetries, these are also negligible. The most important effect is to introduce a term which violates h-particle conservation:

$$H^{nnn}_{\rm eff} = \sum_{\langle\langle ij\rangle\rangle} y[h_i h_j(\vec{O}^{t\dagger}_{a;ij}\cdot\vec{O}^{t\dagger}_{b;ij} + O^{s\dagger}_{a;ij}O^{s\dagger}_{b;ij}) + \text{H.c.}]. \tag{10}$$

Here $\vec{O}^{t\dagger}_{a/b;ij}$ creates a triplet of spin-1 states of a/b particles on the pair of sites ij, $O^{s\dagger}_{a/b;ij}$ creates a singlet of a/b particles on this pair, and the ''fugacity'' $y = 2t_{ab}^2/V$. Note that although Eq. (10) violates conservation of the number of ''holes,'' it creates and annihilates them only in pairs. There thus remains a conserved Ising charge or parity $[=\Sigma_i h_i^\dagger h_i \ (\text{mod } 2)]$, signifying whether the number of holes is even or odd. This parity can be traced back to fact that the two orbitals on each site transform differently under spatial reflections.

B. Pseudospin description

To understand the behavior of this model, we now introduce a useful reformulation. Formally, the five possible states on each site can be viewed as different quantized values of a generalized pseudospin, and the above terms then take the form of nearest-neighbor interactions between these spins. In particular, we define five states per site via $|1\rangle = a_\uparrow^\dagger b_\uparrow^\dagger|v\rangle$, $|2\rangle = a_\uparrow^\dagger b_\downarrow^\dagger|v\rangle$, $|3\rangle = a_\downarrow^\dagger b_\uparrow^\dagger|v\rangle$, $|4\rangle = a_\downarrow^\dagger b_\downarrow^\dagger|v\rangle$, and $|5\rangle = b_\uparrow^\dagger b_\downarrow^\dagger|v\rangle$. The Hamiltonian can be rewritten in terms of 5×5 spin matrices $\mathcal{T}^{\mu\nu}$, where $\langle\mu'|\mathcal{T}^{\mu\nu}|\nu'\rangle = \delta^{\mu\mu'}\delta^{\nu\nu'}$. Neglecting for the moment the hole-non-conserving terms in Eq. (10), $H^h_{\rm eff} = H^{ps}_{\rm eff} + \text{const}$, where

$$H^{ps}_{\rm eff} = \sum_{\langle ij\rangle} \frac{\mathcal{J}_\perp}{2} \sum_{\mu=1}^{4} (\mathcal{T}_i^{\mu 5}\mathcal{T}_j^{5\mu} + i\leftrightarrow j) + \mathcal{J}_z \mathcal{T}_i^z \mathcal{T}_j^z - \mathcal{H}\sum_i \mathcal{T}_i^z , \tag{11}$$

and $\mathcal{T}_i^z = (\Sigma_{\mu=1}^4 \mathcal{T}_i^{\mu\mu} - \mathcal{T}_i^{55})/2$. The generalized exchange constants $\mathcal{J}_\perp = 2t_h$, $\mathcal{J}_z = V_{hh}$, and Zeeman field $\mathcal{H} = dV_{hh}/2 - \mu_h$.

This form of the Hamiltonian exposes a strong similarity to the spin-1/2 XXZ model in a Zeeman field. In particular, the ''boson hopping'' $\mathcal{J}_\perp$ is analogous to an antiferromagnetic in-plane exchange ($S_i^+ S_j^-$ terms), spin-boson interaction $\mathcal{J}^z$ to an antiferromagnetic Ising exchange, and $\mathcal{H}$ to a z-axis field. For $\mathcal{J}_\perp \gg \mathcal{J}_z$ and $\mathcal{H}$ not too large, one expects the analog of canted XY antiferromagnetism, while for $\mathcal{J}_z \gg \mathcal{J}_\perp$, one instead expects z-axis Ising antiferromagnetism up to a threshold value of $|\mathcal{H}|$. For large fields, $|\mathcal{H}| \gg \mathcal{J}_\perp, \mathcal{J}_z$, one ultimately expects fully polarized states, which correspond to the Mott and band insulators for $\mathcal{H} > 0$ and $\mathcal{H} < 0$, respectively.

Surprisingly, $H^{ps}_{\rm eff}$ displays an enormous SU(4) invariance under $T^{5\mu} \to \Sigma_{\nu=1}^4 U_{\mu\nu} T^{5\nu}$ and $T^{\mu 5} \to \Sigma_{\nu=1}^4 U^*_{\mu\nu} T^{\nu 5}$, where U is an SU(4) matrix. SU(4) symmetry is expected to be a good approximation over a range of energies, because in the physical limits $V \ll U \sim E_G$ and $J_H \ll J \ll \mathcal{J}_\perp, \mathcal{J}_z, \mathcal{H}$. Thus we will take the approach of first solving the SU(4) invariant model, and considering successively the exchanges J and J_H, which reduce the symmetry of $H_{\rm eff}$ to SU(2)×SU(2) (independent *physical* spin rotations of the a and b moments) and SU(2)×U(1), respectively.

Finally, we consider the effects of the hole-pair creation and annihilation terms in Eq. (10), which can also be transcribed into the pseudo-spin language. One finds $H^{ps}_{\rm eff} \to H^{ps}_{\rm eff} + H^I_{\rm eff}$, where

$$H^I_{\rm eff} = \sum_{\langle\langle ij\rangle\rangle} \mathcal{J}_I[\mathcal{T}_i^{25}\mathcal{T}_j^{25} + \mathcal{T}_i^{35}\mathcal{T}_j^{35} - \mathcal{T}_i^{15}\mathcal{T}_j^{45} - \mathcal{T}_i^{45}\mathcal{T}_j^{15} + \mathcal{T}_i^{52}\mathcal{T}_j^{52} + \mathcal{T}_i^{53}\mathcal{T}_j^{53} - \mathcal{T}_i^{51}\mathcal{T}_j^{54} - \mathcal{T}_i^{54}\mathcal{T}_j^{51}]. \tag{12}$$

The coupling $\mathcal{J}_I \propto y$. While it is perhaps not completely transparent in this notation [a better notation for this term will be introduced in Sec. III C—see Eq. (19)], the effect of $H^I_{\rm eff}$ is to further break the SU(2)×U(1) symmetry down to SU(2)×Z_2. The Z_2 invariance is the remnant of the physical parity symmetry discussed in Sec. III A.

C. Mean-field theory and undoped phase diagram

We expect that a simple Weiss mean-field theory (MFT) gives qualitatively correct results for the stoichiometric phase diagram, as it does for the ordinary XXZ+Zeeman model.[16] Neglecting $H^s_{\rm eff}$, the MFT consists of replacing

$$T_i^{\mu 5}T_j^{5\mu} \to \langle T_i^{\mu 5}\rangle T_j^{5\mu} + T_i^{\mu 5}\langle T_j^{5\mu}\rangle - \langle T_i^{\mu 5}\rangle\langle T_j^{5\mu}\rangle, \tag{13}$$

for each bond i and j on the lattice, and similarly for the $T_i^z T_j^z$ interaction. With this replacement, the Hamiltonian decouples on different lattice sites, and the problem reduces to solving the appropriate single-site problems self-consistently. As an antiferromagnetic solution is expected, this amounts to equations for the (eight-component) transverse staggered magnetization, defined by $\langle T_i^{\mu 5}\rangle =$

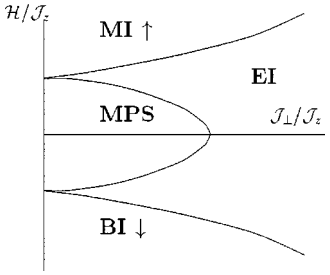

FIG. 4. Mean-field phase diagram of the fully SU(4)-invariant pseudospin model. A large pseudo-Zeeman field (which scales linearly with the orbital splitting E_G) stabilizes either the Mott insulating (MI) or band insulating (BI) state, depending upon its sign. For ''in-plane'' anisotropy ($\mathcal{J}_\perp > \mathcal{J}_z$), the intervening phase is an excitonic insulator (EI). In the opposite limit (''Ising'' anisotropy) it consists of a micro-phase-separated state with a checkerboard pattern of alternating band and Mott insulating configurations at the lattice scale. In obtaining the pseudospin model from the strong-coupling limit of Eqs. (4)–(6), one finds in-plane anisotropy, and the intermediate state is expected to be excitonically ordered.

$(-1)^i[n_\perp^{2\mu-1} + i n_\perp^{2\mu}]$, and the uniform and staggered z-axis magnetizations, defined by $\langle T_i^z \rangle = m_z + (-1)^i n_z$. Because of SU(4) symmetry, all orientations of $n_\perp^k$ are degenerate, and it is sufficient to assume $n_\perp^k \equiv n_\perp \delta^{k1}$. In this subspace, the equations of MFT become *identical* to those of the conventional spin-1/2 XXZ antiferromagnet in a Zeeman field. These equations were solved in Ref. 17. The resulting phase diagram is shown in Fig. 4.

Since $\mathcal{J}_\perp > \mathcal{J}_z$, we expect a transverse pseudospin polarization, $\langle \mathcal{T}^{\mu 5} \rangle \neq 0$, provided $|\mathcal{H}| < \mathcal{H}_c = d\mathcal{J}_\perp$. Remarkably, the transverse components of the pseudospin operator are exactly the excitonic order parameters. In particular, straightforward algebra shows $\mathcal{T}^{\mu 5} = (-\Delta_{\uparrow\downarrow}, \Delta_{\uparrow\uparrow}, -\Delta_{\downarrow\downarrow}, \Delta_{\downarrow\uparrow})$. Thus for $\mathcal{J}_\perp > \mathcal{J}_z$, MFT predicts an excitonic insulator.

We now turn to the evolution of the ground state in this regime on introducing the symmetry-breaking terms in $H_{\rm eff}^S$. In their absence, the excitonic order parameter can ''point'' in any direction which is equivalent under the broken SU(4) symmetry. Within MFT, this amounts to complete freedom to choose the four complex components of $\Delta_{\alpha\beta}$, subject to the constraint $\mathrm{Tr}\,\Delta^\dagger\Delta = \frac{1}{4}(1 - \mathcal{H}^2/\mathcal{H}_c^2) \equiv \Delta_0^2/2$. In term of singlet and triplet components defined by Eq. (2), this constraint simply implies $|\Delta_s|^2 + \vec{\Delta}_t^* \cdot \vec{\Delta}_t = \Delta_0^2$. The perturbations in $H_{\rm eff}^S$ can be viewed as ''anisotropies'' favoring submanifolds within this space.

To clarify the nature of the anisotropy terms, it is helpful to work with the mean-field wave function, $|\Psi_0\rangle = \Pi_i \mathcal{E}_i^\dagger |BI\rangle$, where $|BI\rangle = \Pi_i b_{i\uparrow}^\dagger b_{i\downarrow} |v\rangle$ is the noninteracting band-insulating state, and

$$\mathcal{E}_i^\dagger = c\left(1 + (-1)^i |c|^{-2} \sum_{\alpha\beta} \Delta_{\alpha\beta}^* a_{i\alpha}^\dagger b_{i\beta}\right) \tag{14}$$

is a local ''exciton creation operator.'' Here $|c|^2 = (1 - \mathcal{H}/\mathcal{H}_c)/2$. It is now straightforward to evaluate the expectation value of $H_{\rm eff}^S$ in the mean-field ground state. Up to a constant for fixed $\mathrm{Tr}\,\Delta^\dagger\Delta$, on a hypercubic lattice one finds the bulk energy density

$$\epsilon_b \equiv L^{-d}\langle H_{\rm eff}^S \rangle = 2\tilde{J}\,\mathrm{Tr}(\Delta^\dagger\Delta)^2 + \tilde{J}_H |\mathrm{Tr}\,\Delta|^2, \tag{15}$$

where $\tilde{J} = d a^{-d} J/2|c|^4$ and $\tilde{J}_H = a^{-d} J_H/2|c|^2$. The above terms are essentially completely determined by the SU(2) $\times$ SU(2) and SU(2) $\times$ U(1) symmetries. To proceed, we employ two identities derivable from Eq. (2):

$$\mathrm{Tr}(\Delta^\dagger\Delta)^2 = \frac{1}{8}(\Delta_s^*\Delta_s + \vec{\Delta}_t^* \cdot \vec{\Delta}_t)^2 + \frac{1}{8}|\Delta_s^* \vec{\Delta}_t + \Delta_s \vec{\Delta}_t^* - i\vec{\Delta}_t \wedge \vec{\Delta}_t^*|^2, \tag{16}$$

$$\mathrm{Tr}\,\Delta = \Delta_s. \tag{17}$$

By assumption, $J \gg J_H$, so that the first term in Eq. (15) creates the dominant splitting of the SU(4) ground-state degeneracy. The low-energy submanifold thus consists of order parameters which minimize $\mathrm{Tr}(\Delta^\dagger\Delta)^2$. Equation (16) then implies $\Delta_s^* \vec{\Delta}_t + \Delta_s \vec{\Delta}_t^* - i\vec{\Delta}_t \wedge \vec{\Delta}_t^* = 0$ [note that the first term in Eq. (16) is constant and equal to $\Delta_0^2/8$]. The physical content of this condition is made clear by calculating the mean spin polarization on the a site using the mean-field wave function in Eq. (14):

$$\vec{s}_a = \langle \vec{S}_a \rangle = \frac{1}{4|c|^2}(i\vec{\Delta}_t \wedge \vec{\Delta}_t^* + \Delta_s^* \vec{\Delta}_t + \Delta_s \vec{\Delta}_t^*). \tag{18}$$

Thus the influence of the exchange coupling J is to favor states with $\vec{s}_a = 0$.

This condition still allows a fairly large range of states, the simplest of which are pure singlet ($|\Delta_s| = \Delta_0$, $\vec{\Delta}_t = 0$) and pure collinear triplet ($\Delta_s = 0$, $\vec{\Delta}_t \neq 0$, $\vec{\Delta}_t \wedge \vec{\Delta}_t^* = 0$) orderings. The additional effect of the Hunds-rule ferromagnetic coupling J_H is to introduce a small extra ''mass'' for the singlet order parameter, favoring a pure triplet state.

The *phase* of the triplet order parameter is determined by the ''Ising anisotropy'' terms in Eq. (12). To see this, we rewrite $\mathcal{T}^{\mu 5}$ and $\mathcal{T}^{5\mu}$ directly in terms of Δ. One finds

$$H_{\rm eff}^I = \sum_{\langle\langle ij \rangle\rangle} \mathcal{J}_I\,\mathrm{Tr}(\Delta_i \Delta_j + \Delta_j^\dagger \Delta_i^\dagger). \tag{19}$$

Note that Eq. (19) explicitly breaks the U(1) symmetry of phase rotations of Δ, down to the Ising invariance $\Delta \to -\Delta$. If $H_{\rm eff}^I$ is considered a weak perturbation, it can be treated by simply evaluating its expectation value in the mean-field ground state [Eq. (14)], giving $\langle \Delta_i \rangle = \langle \Delta_j \rangle = \Delta$, since i and j are next-nearest neighbors. Using $\mathrm{Tr}\,\Delta^2 = (\Delta_s^2 + \vec{\Delta}_t \cdot \vec{\Delta}_t)/2$, one finds (since $\mathcal{J}^I > 0$) that Eq. (19) favors an *imaginary* triplet order parameter $\vec{\Delta}_t = -\vec{\Delta}_t^*$. This is *different* from the weak-coupling treatment of Ref. 6, in which a *real* triplet order parameter was found to be preferred.

Unlike in superconductivity, the phase of the excitonic order parameter has physical significance, as discussed by Halperin and Rice.[3] In particular, it is straightforward to show that a *real* $\vec{\Delta}_t$ order parameter corresponds to a nonzero average spin density within the unit cell of the crystal, while for $\vec{\Delta}_t$ imaginary, the spin density is zero but there are instead nonzero spin *currents*. The imaginary triplet state ob-

tained here is therefore a sort of spin ''flux phase'' with nonzero spin currents. See Sec. V for a more in-depth discussion.

Apart from this difference, the strong-coupling results of this section are in very close agreement with the weak-coupling results of Ref. 6. Indeed, not too much significance should be attached to the difference in phase of the order parameters, as indeed the models are in any case not completely identical. In fact, the detailed correspondence of results up to this point strongly argues for a continuous smooth interpolation (''adiabatic continuity'') of most physical properties of such systems as the overall interaction strength is increased from small to large values.

Finally, we comment on the modifications to the SU(4)-invariant phase diagram in the presence of the symmetry-breaking terms in Eqs. (8) and (10). As argued above, these favor an imaginary triplet state when $\mathcal{H}=0$. Inside the Mott insulator, these terms stabilize an antiferromagnetically ordered magnetic state. On approaching the Mott insulator boundary, therefore, we expect the emergence of magnetic ordering. This implies the existence of at least one additional phase boundary separating the triplet EI (which has no nonzero spin density) from a magnetically ordered EI with nonzero average spin density, somewhere inside the region in which the EI phase occurs in the SU(4)-invariant model.

IV. DOPING

In this section, we consider the behavior as a low density of electrons is added to the system. In the strong-coupling limit, this reduces to an effective t-J-like model, in which the Hilbert space is restricted to states in which all sites (unit cells) are either doubly (corresponding to the excitonic pseudospins modeled above) or triply occupied, the latter containing one a and two b electrons. The system is then governed by an effective Hamiltonian $H_{\rm dope}=H^{s}_{\rm eff}+H^{ps}_{\rm eff}+\tilde{\mathcal{P}}H'\tilde{\mathcal{P}}$, where $\tilde{\mathcal{P}}$ projects onto this restricted Hilbert space.

As many years of work on high-T_c superconductivity has taught us, the problem of doping a correlated (Mott) insulator, particularly with spin (and here pseudospin) ordering, is extremely complex and difficult. Here, we will adopt the absolute simplest approach extending the above MFT to the low-electron-density limit. We assume, as suggested by the weak-coupling analysis, that the essential ingredient for excitonic ferromagnetism is the approximate enhanced [in this case SU(4)] symmetry of the effective Hamiltonian. In considering the doped state, then, it is crucial to determine in what way the added electrons affect the splitting of the degenerate SU(4) ground-state manifold.

A. Variational treatment for a single electron

In the strong-coupling limit, the majority of the energy of an added electron is kinetic, since $t\gg\mathcal{J},\mathcal{J}_\perp\sim t^2/V$, etc.. Just as in the simpler but much studied t–J model for the cuprates, coherent motion of an added electron, however, is greatly hindered by (pseudo)-spin ordering of the insulating background. Moreover, coherent motion is possible to a varying degree depending upon the precise nature of the background. We first consider this effect for a single added electron using the variational method. A natural variational ansatz is

$$|\Psi_1\rangle=\sum_{i\alpha}\psi_{i\alpha}a^\dagger_{i\alpha}\prod_{j\neq i}\mathcal{E}^\dagger_j|BI\rangle, \tag{20}$$

where *both* the doped electron's wave function $\psi_{i\alpha}$ and the excitonic order parameter $\Delta_{\alpha\beta}$ (implicit in $\mathcal{E}^\dagger_j$) are considered as variational parameters. For fixed $\mathrm{Tr}\,\Delta^\dagger\Delta$, the energy depends only upon J, J_H, and t. In particular, one finds

$$\epsilon_v=L^{-d}\langle\Psi_1|H_{\rm dope}|\Psi_1\rangle=\epsilon_b[1-2d(a_0/L)^d]+L^{-d}\epsilon_e, \tag{21}$$

where a_0 is the lattice spacing,

$$\epsilon_e=t\sum_{\langle ij\rangle}\psi^*_{i\alpha}\hat{T}_{\alpha\beta}\psi_{j\beta}, \tag{22}$$

and the matrix $\hat{T}_{\alpha\beta}=|c|^2\delta_{\alpha\beta}+|c|^{-2}(\Delta\Delta^\dagger)_{\alpha\beta}$. Physically, we identify the first term in Eq. (21) as the bulk energy density, reduced by the presence of a single doped electron [occupying the volume fraction $(a/L)^d$]. In the second term, the quantity ϵ_e is then readily interpreted as the energy of the added electron. Equation (22) is then a hopping Hamiltonian for this electron. In a polarized excitonic background, this hopping is in general nondiagonal in spin. In terms of singlet and triplet components,

$$\hat{T}=\frac{(1+|c|^2)}{2}+\vec{s}_a\cdot\vec{\sigma}^*, \tag{23}$$

where $\vec{s}_a$, the mean spin polarization on the a site, is given by Eq. (18). Minimizing Eq. (22) in the space of normalized wave functions $\psi_{i\alpha}$ gives the tight-binding Schrödinger equation,

$$t\sum_{\langle ji\rangle}\sum_{\beta}\hat{T}_{\alpha\beta}\psi_{j\beta}=\epsilon_e\psi_{i\alpha}, \tag{24}$$

where the angular brackets indicate a sum over the nearest neighbors j of site i. The single-particle eigenstates of this equation are plane waves with spins polarized parallel and antiparallel to $\vec{s}_a$, with eigenvalues

$$\epsilon_{e\pm}(\mathbf{k})=2t\left[\frac{1+|c|^2}{2}\pm|\vec{s}_a|\right]\sum_{i=1}^{d}[\cos k_i a_0], \tag{25}$$

where a_0 is the lattice spacing. The location of the minimum-energy electronic excitations depends crucially on the magnitude of $\vec{s}_a$, and hence $\mathcal{H}$. When $\mathcal{H}>\mathcal{H}_c/3$, electrons with spin parallel and antiparallel to $\vec{s}_a$ have minimum energy at different points in momentum space. Such large values of $\mathcal{H}$ correspond to strongly overlapping bands, close to the boundary between the Mott and excitonic insulators. For simplicity, we will specialize to the case when $|\vec{s}_a|<(1+|c|^2)/2$, which occurs for $\mathcal{H}<\mathcal{H}_c/3$. In this case, the minimal energy single-particle energy excitations for both spin orientations have momentum $\mathbf{k}=(\pi,\ldots,\pi)$. Furthermore, the optimal spin orientation is parallel to $\vec{s}_a$. Such an electron takes advantage of the ''Zeeman'' energy due to the exchange field (proportional to $\vec{s}_a$) generated by the ''core'' spins (i.e., the spins of the two electrons per unit cell present in the insulator).

In the undoped system, however, $\vec{s}_a = 0$, due to the anisotropy in Eq. (15). We therefore expect that the optimal order parameter in the doped system is determined by a competition between these two terms. With some algebra, it is straightforward to verify that, due to the Hunds-rule term J_H, the complex pure triplet state (i.e., with $\vec{\Delta}_t \wedge \vec{\Delta}_t^* \neq 0$, but $\Delta_s = 0$) is always more energetically favorable than a singlet-triplet coexistence (with $\mathrm{Re}\,\Delta_s^* \vec{\Delta}_t \neq 0$).[18] Without loss of generality, it is thus convenient to choose a spin quantization axis, letting

$$\vec{\Delta}_t = \Delta_0(\cos\theta \hat{\mathbf{x}} + i \sin\theta \hat{\mathbf{y}}). \tag{26}$$

One then finds $\vec{s}_a = -(\Delta_0^2/2|c|^2)\sin(2\theta)\hat{\mathbf{z}}$. In any such state, $\vec{s}_b = \vec{s}_a$, so that the core spins also contribute to the ferromagnetic moment.

B. Free Fermi gas approximation

It remains to determine the optimal angle θ. To proceed, we need to extend Eq. (21) to a small but nonzero *density* of doped electrons. At low densities, it seems natural to neglect interactions between doped electrons, and use the simplest possible *free Fermi gas* estimate for the electronic dopant energy. In particular, we approximate the energy of the system as the sum of two contributions: a ''bulk'' contribution from the undoped unit cells containing two electrons and a spatially uniform order parameter $\Delta_{\alpha\beta}$, and a ''dopant'' contribution, approximated by the energy of a free Fermi gas of electrons with dispersion given by Eq. (25). For concreteness, the detailed formulas are presented in the following for three spatial dimensions ($d=3$). At low densities, only single-particle states near $\mathbf{k} = \boldsymbol{\pi} = (\pi, \pi, \pi)$ are occupied, so it is convenient to expand around this point, $\mathbf{k} = \boldsymbol{\pi} + \mathbf{q}$, yielding the dispersion

$$\epsilon_{e\pm}(\mathbf{q}) = -2t\left[\frac{(1+|c|^2)}{2} \pm |\vec{s}_a|\right]\left[3 - \frac{q^2 a_0^2}{2}\right] - \tilde{\mu}. \tag{27}$$

Here we have reinstated a (shifted) chemical potential $\tilde{\mu}$ to control the density of doped electrons. It is both convenient and physically helpful to work at fixed chemical potential rather than fixed charge density, as this naturally allows for the possibility of phase separation. As is perhaps not surprising based on the results of weak-coupling analysis,[6,7] we will see that phase separation does indeed occur in a physically interesting parameter range of the model (at least within this approximation).

Because we are interested in the energy density only insofar as to determine the angle θ, we neglect in the following all terms independent of θ. Inserting Eq. (26) into Eq. (15) gives the bulk energy

$$\epsilon_b = [3J\Delta_0^4/(8a_0^3|c|^4)]\sin^2 2\theta + \mathrm{const} \tag{28}$$

(in three dimensions). This must be added to the ground-state energy of the free Fermi gas of doped electrons. Simple but tedious algebraic calculations lead to the final expression for the total energy density of the system,

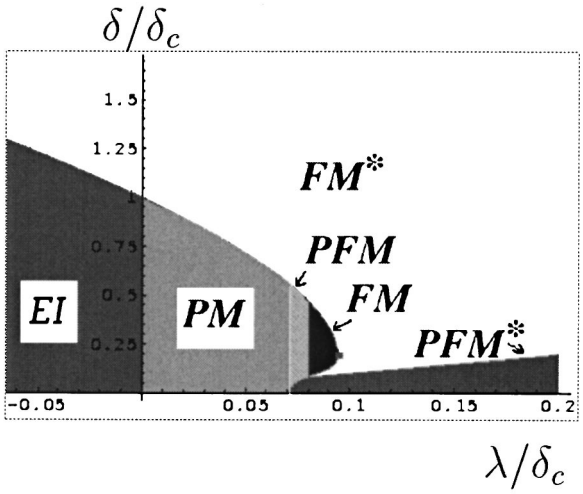

FIG. 5. Free Fermi gas approximation of the zero-temperature phase diagram. The abscissa λ/δ_c is the nondimensionalized chemical potential, and the ordinate δ/δ_c indicates the strength of excitonic ordering relative to superexchange interactions [see Eqs. (29)–(35) for precise definitions]. The properties of the various phases shown are listed in Table I. For larger λ (not shown), both excitonic ordering and ferromagnetism disappear, owing to the reduction of the amplitude of Δ.

$$\epsilon_f = \bar{\epsilon}\delta^2\left[g^2 - \sqrt{\frac{\delta}{\delta_c}}\mathcal{E}(g,\gamma)\right], \tag{29}$$

where

$$\bar{\epsilon} = \frac{3J(1+|c|^2)^2}{8a^3}, \tag{30}$$

$$\delta = \frac{\Delta_0^2}{|c|^2(1+|c|^2)}, \tag{31}$$

$$\delta_c = \left(\frac{5\pi^2(1+|c|^2)}{16\sqrt{6}}\frac{J}{t}\right)^2, \tag{32}$$

$$g = \sin 2\theta, \tag{33}$$

$$\lambda = 1 + \frac{\tilde{\mu}}{3t(1+|c|^2)}, \tag{34}$$

$$\gamma = \lambda/\delta. \tag{35}$$

The function $\mathcal{E}(g,\gamma)$ is straightforwardly related to the energy density of the three-dimensional free-electron gas in a Zeeman field. In general it depends not only on g and γ, but also on δ. For simplicity, we will assume $|\delta g| \ll 1$, which holds near to the excitonic insulator-band insulator boundary, and is satisfied more generally in the interesting region of the phase diagram [where δ is $O(\delta_c)$, since $\delta_c \ll 1$ in the strong-coupling limit $J/t \ll 1$—see Fig. 5]. In this case, $\mathcal{E}(g,\gamma)$ becomes independent of δ. Its functional form is

$$\mathcal{E}(g,\gamma) = \sum_{z=\pm 1} (\gamma + zg)^{5/2}\Theta(\gamma + zg), \tag{36}$$

TABLE I. Phases of the doped EI in the free-Fermi-gas approximation. The five columns list the abbreviation, the presence or absence of doping, the magnetic order, the degree of polarization, and the excitonic angle (θ), respectively, for the six phases.

Phase	Doped?	Mag.	Pol.	Angle
EI	no	para	n/a	$\theta=0$
PM	yes	para	n/a	$\theta=0$
PFM	yes	ferro	partial	$0<\theta<\pi/4$
FM	yes	ferro	full	$0<\theta<\pi/4$
PFM*	yes	ferro	partial	$\theta=\pi/4$
FM*	yes	ferro	full	$\theta=\pi/4$

where $\Theta(\gamma)$ is the Heaviside step function. Equations (29)–(36) give the energy density of the system as a function of chemical potential $\tilde{\mu}$ (through γ) and order parameter angle θ (through g). The optimal excitonic angle θ is determined by minimizing $\epsilon(\tilde{\mu},\theta)$ at fixed $\tilde{\mu}$. If $\tilde{\mu}$ and θ are known, the density of doped electrons x and itinerant magnetization density m_{it} are then given by the free-fermion results:

$$x=\sqrt{\frac{2}{6\pi^2a^3}}\sum_{z=\pm1}(\gamma+zg)^{3/2}\Theta(\gamma+zg), \tag{37}$$

$$m_{it}=\frac{1}{6\sqrt{2}\pi^2a^3}\sum_{z=\pm1}z(\gamma+zg)^{3/2}\Theta(\gamma+zg). \tag{38}$$

Note that the system is doped (i.e., $x\neq0$) whenever $\gamma+|g|>0$. One should also keep in mind that the full magnetization density $m=m_{it}+m_{core}$ includes a contribution $m_{core}=-(\Delta_0^2/|c|^2a^3)\sin(2\theta)$ from the core spins.

Equations (29)–(38) completely determine the state of the system at zero-temperature as a function of λ and δ. The mathematical problem of minimizing ϵ_f is algebraically quite tedious, and significant care must be taken to avoid spurious local minima and saddle points. The results of a careful study are shown in Fig. 5. All the phases shown are excitonically ordered, but differ in doping x, excitonic angle θ, and magnetization m. The properties of each are summarized in Table I. In the strong-coupling limit, we expect (see Sec. IV) $\delta/\delta_c\gg1$, in which case there is a direct *first-order* transition from a paramagnetic excitonic insulator to a fully-polarized ferromagnetic metal (FMFP*).

The phase boundaries in Fig. 5 variously indicate first (discontinuous) and second(discontinuous) order transitions. All the vertical phase boundaries denote continuous transitions, while most of the transitions on curved phase boundaries are discontinuous. The exceptions are the PPFM*-FPFM* boundary (which is everywhere second order) and the lower portion of the FPFM-FPFM* transition line, which is continuous below the tricritical point indicated in the figure.

Which portion of this phase diagram is most physically significant? In the strong-coupling limit, $\delta_c\ll1$, and it therefore seems reasonable to suppose $\delta/\delta_c\gg1$, so that the system undergoes a simple and direct first-order transition from the undoped and paramagnetic EI to the fully-rotated half-metallic ferromagnet, FPFM*. Coincident with this transition is a jump in the electronic charge density x, from zero in the insulator to a nonzero value in the metal.

V. DISCUSSION

A. Symmetries and properties of excitonic insulators

The model introduced in Sec. II contains many possible excitonically ordered states in various regions of its phase diagram. In the undoped case, we have argued that a simple paramagnetic collinear triplet ordering is most likely, while a state with $\vec{\Delta}_t\wedge\vec{\Delta}_t^*\neq0$ is obtained for electron densities slightly greater than two per unit cell. Nevertheless, if, as supposed, SU(4) symmetry is a good approximation, then many other possible states must necessarily be nearly as low in energy. In the hope that the truth may ultimately be decided by experimental measurements, it seems useful to delineate the physical characteristics of each of these phases.

With the exception of the noncollinearly ordered states, the analysis of the next few paragraphs is identical (though in somewhat different notation) to that of Halperin and Rice.[3] First, let us consider the existence of a time-averaged magnetic moment. In the tight-binding formulation, the electron field operator is expanded in terms of Wannier orbitals,

$$\psi_\alpha(\mathbf{r})=\sum_i[\phi_a(\mathbf{r}-\mathbf{R}_i)a_{i\alpha}+\phi_b(\mathbf{r}-\mathbf{R}_i)b_{i\alpha}], \tag{39}$$

where $\phi_{a/b}(\mathbf{r})$ is the Wannier function for the a/b orbital, and we neglect the other (unoccupied) states. Consider next the spin-density operator. We will assume for simplicity (though this is not essential) that each Wannier function has support only within one unit cell. Equation (39) then leads to a representation for the spin-density operator $\vec{S}$:

$$2\vec{S}(\mathbf{r})=\psi^\dagger\vec{\sigma}\psi, \tag{40}$$

$$=|\phi_a(\mathbf{r})|^2\langle a^\dagger\vec{\sigma}a\rangle+|\phi_b(\mathbf{r})|^2\langle b^\dagger\vec{\sigma}b\rangle + \phi_a^*(\mathbf{r})\phi_b(\mathbf{r})\langle a^\dagger\vec{\sigma}b\rangle+\phi_b^*(\mathbf{r})\phi_a(\mathbf{r})\langle b^\dagger\vec{\sigma}a\rangle. \tag{41}$$

To proceed, we choose both Wannier functions to be *real*. Then *for the undoped case*, the spin density can be rewritten in terms of $\vec{s}_{a/b}$ and $\vec{\Delta}_t$:

$$\vec{S}(\mathbf{r})=|\phi_a(\mathbf{r})|^2\vec{s}_a+|\phi_b(\mathbf{r})|^2\vec{s}_b+2\phi_a(\mathbf{r})\phi_b(\mathbf{r})\mathrm{Re}\,\vec{\Delta}_t. \tag{42}$$

Further recall Eq. (18) and its analog for $\vec{s}_b$:

$$\vec{s}_{a/b}=\frac{1}{4|c|^2}[i\vec{\Delta}_t\wedge\vec{\Delta}_t^*\pm(\Delta_s^*\vec{\Delta}_t+\Delta_s\vec{\Delta}_t^*)]. \tag{43}$$

There are thus nonzero static local moments whenever $\mathrm{Re}\,\Delta_s^*\vec{\Delta}_t$, $\mathrm{Im}\,\vec{\Delta}_t\wedge\vec{\Delta}_t^*$, or $\mathrm{Re}\,\vec{\Delta}_t$ are nonzero. In the simplest such states, $\vec{\Delta}_t=|\vec{\Delta}_t|\hat{e}$, where $\hat{e}$ is a real unit vector. In this case, there is a spatially varying static moment within the unit cell oriented along the $\hat{e}$ axis. The *net* moment (integrated over the unit cell) is, however, zero, unless $\vec{\Delta}_t\wedge\vec{\Delta}_t^*\neq0$, in which case the real and imaginary parts of $\vec{\Delta}_t$ are both nonzero and not parallel. In addition to the net ferromagnetic polarization along $\mathrm{Im}\,\vec{\Delta}_t\wedge\vec{\Delta}_t^*$, such states have a

noncollinear static spin density in the unit cell. The net moment along these other directions remains zero. To see why such states sustain a net polarization, consider the particular case given in Eq. (26), with excitonic angle θ. One can then use Eq. (2) to rewrite the order-parameter matrix as

$$\Delta = \frac{\Delta_0}{2}[(\cos\theta + \sin\theta)\sigma^+ + (\cos\theta - \sin\theta)\sigma^-]. \quad (44)$$

Inspection of the mean-field wave function [Eqs. (14) and (44)] immediately shows that the amplitude for up- and down-spins are unequal, so long as θ is not a multiple of π.

Some confusion may arise in the reader with regard to time-reversal symmetry. It appears surprising to have $\vec{\Delta}_t$ and $i\vec{\Delta}_t \wedge \vec{\Delta}_t^*$, the latter containing a cross product, both contributing to $\vec{s}_{a/b}$. In fact, both terms transform like a spin under time reversal. This is simplest to see in the path-integral representation of the quantum system, in which the fermion operators are replaced by time-dependent Grassman fields $a_\alpha \to a_\alpha(t)$, $a_\alpha^\dagger \to \overline{a}_\alpha(t)$, and similarly for $b_\alpha, b_\alpha^\dagger$. The Grassman fields then transform under time-reversal according to

$$a_\alpha(t) \to \sigma^y_{\alpha\beta}\overline{a}_\beta(-t), \quad (45)$$

$$\overline{a}_\alpha(t) \to -\sigma^y_{\alpha\beta}a_\beta(-t), \quad (46)$$

$$b_\alpha(t) \to \sigma^y_{\alpha\beta}\overline{b}_\beta(-t), \quad (47)$$

$$\overline{b}_\alpha(t) \to -\sigma^y_{\alpha\beta}b_\beta(-t). \quad (48)$$

Note the important minus sign in the above transformation, which is possible because a_α and $\overline{a}_\alpha$ (b_α and $\overline{b}_\alpha$) are independent fields (not related by complex conjugation) in the path integral. This reflects the antiunitary nature of time-reversal symmetry. At any rate, Eqs. (1) and (2) then imply that

$$\Delta_s \to \Delta_s^*, \quad (49)$$

$$\vec{\Delta}_t \to -\vec{\Delta}_t^* \quad (50)$$

under time reversal. The combination of complex conjugation and the minus sign for $\vec{\Delta}_t$ imply that both terms in Eq. (43) are odd under time reversal. Indeed, the necessary and sufficient conditions for broken time-reversal symmetry is $\mathrm{Re}\langle\vec{\Delta}_t\rangle \neq 0$ and/or $\mathrm{Im}\langle\Delta_s\rangle \neq 0$.

A perhaps surprising consequence of Eq. (41) is that apparently if $\mathrm{Re}\,\Delta_s^*\vec{\Delta}_t \neq 0$ but $\mathrm{Im}\,\vec{\Delta}_t \wedge \vec{\Delta}_t^* = 0$, there is no net magnetization. In fact, this result applies only to the particular undoped model considered here, and is a consequence of a special variety of particle-hole symmetry (which we denote PH). To make this explicit, define a hole creation operator $\tilde{b}_\alpha^\dagger = \sigma^y_{\alpha\beta}b_\beta$. Then the electron number operator can be rewritten as

$$n = a^\dagger a + b^\dagger b = 2 + a^\dagger a - \tilde{b}^\dagger\tilde{b}. \quad (51)$$

In the undoped system, the mean number of electrons per unit cell is two, so that $\langle a^\dagger a - \tilde{b}^\dagger\tilde{b}\rangle = 0$. Thus precisely at this density, and *only* at this density, we may entertain the possibility of symmetry under the transformation PH:

$$a_\alpha \to_{PH} \tilde{b}_\alpha, \quad \tilde{b}_\alpha \to_{PH} a_\alpha. \quad (52)$$

In the new variables, the excitonic order parameter becomes $\Delta = a_\alpha^\dagger\sigma^y_{\alpha\beta}\tilde{b}_\beta^\dagger$. Thus $\Delta \to -\Delta^T$ (here the superscript T indicates the matrix transpose) under PH. Also useful is the operator $a^\dagger a - b^\dagger b = a^\dagger b + \tilde{b}^\dagger\tilde{b} - 2$ (proportional to $\mathcal{T}^z$ in the $n=2$ subspace), which is invariant under PH. Thus H_{eff}^{ps} [see Eq. (11)] is PH invariant. Similarly, it is straightforward to show that under PH, the two spin operators are exchanged:

$$\vec{S}_a \leftrightarrow_{PH} \vec{S}_b. \quad (53)$$

Thus H_{eff}^s is also PH invariant, as is H_{eff}^I, as can be easily shown. Thus the undoped Hamiltonian is invariant under PH. Considering the order parameters, we find that

$$\Delta_s \to_{PH} \Delta_s, \quad (54)$$

$$\vec{\Delta}_t \to_{PH} -\vec{\Delta}_t. \quad (55)$$

Thus the combination $\mathrm{Re}\,\Delta_s^*\vec{\Delta}_t$ is *odd* under PH, and hence cannot give rise to a total moment, since $\vec{S}_{\mathrm{TOT}}$ is PH invariant. $\mathrm{Im}\,\vec{\Delta}_t \wedge \vec{\Delta}_t^*$, however, is PH invariant, and can hence couple directly to a ferromagnetic moment.

It should be stressed that PH *is not a microscopically exact symmetry*, even in the stoichiometric situation. It occurred in the above analysis only because of the arbitrary choice of equal hopping between a and b orbitals, $t_a = t_b = t$, in Eq. (6). In general, one expects $t_a \neq t_b$, which leads to different antiferromagnetic exchange constants between a and b spins in H_{eff}^s [Eq. (8)]. Different exchange constants destroy the invariance of the Hamiltonian under the interchange of a and b spins [Eq. (53)], which is the effect of PH. It is straightforward to show that, when this asymmetry is included in the microscopic Hamiltonian, states with $\mathrm{Re}\,\Delta_s^*\vec{\Delta}_t \neq 0$ are also ferromagnetic. In addition, even in the model with $t_a = t_b$, *doping* breaks the PH symmetry, and gives rise to a ferromagnetic moment in the $\mathrm{Re}\,\Delta_s^*\vec{\Delta}_t \neq 0$ state.

Considerations similar to those above Eq. (41) apply to the electronic charge density (ρ), current density ($\vec{I}$), and spin current density ($J^{\mu\nu}$) operators. One finds

$$\rho(\mathbf{r}) = -e|\phi_a(\mathbf{r})|^2 n_a - e|\phi_b(\mathbf{r})|^2 n_b - 2e\phi_a(\mathbf{r})\phi_b(\mathbf{r})\mathrm{Re}\,\Delta_s,$$

$$\vec{I}(\mathbf{r}) = \frac{e}{m}\mathrm{Im}\,\Delta_s[\phi_a(\mathbf{r})\vec{\nabla}\phi_b(\mathbf{r}) - \phi_b(\mathbf{r})\vec{\nabla}\phi_a(\mathbf{r})], \quad (56)$$

$$J^{\mu\nu}(\mathbf{r}) = \frac{1}{2m}\mathrm{Im}\,\Delta_t^\mu[\phi_a(\mathbf{r})\partial_\nu\phi_b(\mathbf{r}) - \phi_b(\mathbf{r})\partial_\nu\phi_a(\mathbf{r})].$$

In the final equation above, $J^{\mu\nu}$ is the current density for spin polarized along the μ axis propagating in the ν direction. For completeness, the mean-field expressions for the number of a and b particles are

$$n_a = \langle a^\dagger a\rangle = |c|^{-2}\,\mathrm{Tr}\,\Delta^\dagger\Delta, \quad (57)$$

$$n_b = \langle b^\dagger b \rangle = 2 - n_a . \tag{58}$$

From Eqs. (56), we can read off the physical interpretation of the various other types of ordering. If $\mathrm{Im}\,\vec{\Delta}_t \neq 0$, there is a spontaneous *spin current* in the unit cell. This is necessarily the case for any state with $\vec{\Delta}_t \wedge \vec{\Delta}_t^* \neq 0$, which, as discussed above, also exhibits noncollinear static moments. The simpler state with $\vec{\Delta}_t = i|\Delta_t|\hat{e}$ has *only* the spin currents, and is the magnetic analog of a ''flux phase'' in modern terminology. Similarly, if the singlet order parameter has an imaginary part $\mathrm{Im}\,\Delta_s \neq 0$, there are nonzero charge currents within the unit cell. This is exactly a flux phase. Finally, a real singlet order parameter, $\Delta_s = \Delta_s^* \neq 0$, gives rise to a charge-density $\rho(\mathbf{r})$ that breaks the point group symmetry of the crystal, since $\phi_a(\mathbf{r})\phi_b(\mathbf{r})$ is not a scalar.

Another important characteristic of the phases with triplet ordering is a finite (transverse) uniform spin susceptibility. This is a very general consequence of broken spin-rotational invariance. In the simplest collinear triplet states, $\Delta_t = \Delta_0 e^{i\phi}\hat{e}$, where $\hat{e}$ is a real vector. The elementary excitations of the symmetry-broken state can then be classified *only* by their spin along the triplet axis, $\vec{S}_{\mathrm{TOT}} \cdot \hat{e}$. The transverse components of $\vec{S}_{\mathrm{TOT}}$, however, do not commute with $\vec{\Delta}_t$. An applied Zeeman field along one of these axes therefore immediately acts to mix together the former ground and excited states. It is fairly straightforward to demonstrate by this mechanism a constant transverse spin susceptibility for the collinearly ordered triplet states. For noncollinearly ordered triplets, we conjecture that *all* components of the uniform susceptibility are finite. This distinction is most likely primarily academic, as experimentally available samples would presumably break up into domains with random orientations of $\vec{\Delta}_t$, thus effectively isotropizing the bulk susceptibility. Very crude estimates for the magnitude of χ can be obtained in both the strong- and weak-coupling limits of excitonically ordered states. In strong coupling, the susceptibility can be computed by naive perturbation theory in the mean-field ground state. In the optimal case ($\mathcal{H}=0$), in which the excitonic ordering is maximal, one finds $\chi \sim \mu_B / \mathcal{J}_\perp$, where $\mathcal{J}_\perp \sim t^2/V$ is the characteristic stiffness for excitonic ordering (see Sec. III), and μ_B is the Bohr magneton. In weak coupling, the susceptibility is approximately equal to the free-electron value, $\chi \sim D(\epsilon_F)\mu_B$, where $D(\epsilon_F)$ is the density of states at the Fermi energy.

A puzzling aspect of the experimental data on the hexaborides is the absence of a substantial gap in optical conductivity measurements in the undoped materials. In general, the excitonically ordered insulators discussed here *are* expected to exhibit hard optical gaps [i.e., a complete absence of weight in $\sigma(\omega)$ at small ω] at low frequencies and zero temperature, so this is an important point which such a theory must contend with. Several possible physical situations can, however, resolve this apparent discrepancy. In the weak- and intermediate-coupling limits, it is possible to sustain a metallic state simultaneously with excitonic order. This requires imperfectly nested Fermi surfaces—a detailed investigation of this possibility is underway. Even in the strong-coupling limit, it is also possible that a gap exists, but is anomalously small. Indeed, in the present model, the optical gap can be estimated by considering the energy cost required to transfer an electron from one unit cell to its neighbor. At the optimal conditions for excitonic ordering, one has $U = 2E_G + V$, and a straightforward calculation of energies from Eq. (4) gives the optical gap $\Delta_o \approx V$. Thus one expects at least $\Delta_o \ll U, E_G$. Note that in the strong-coupling limit, there is no universal relation between Δ_o and the excitonic order parameter.

B. Relevance to the hexaborides

The models and discussions in this paper demonstrate the feasibility of a strong-coupling approach to excitonic ordering. A direct application of the results to the hexaborides is, however, not appropriate, due to the simplified nature of the Hamiltonian discussed here. It is possible to generalize the tight-binding model discussed here to a ''two-band'' (p- and d-orbital) Hamiltonian which more accurately models the physics of these materials. This model contains the significant ingredient of orbital degeneracy, and hence considerable additional richness. Such orbital degeneracy is the tight-binding analog of the valley degeneracy encountered in band-theoretic treatments. The *methods* of this paper, however, remain applicable in this case as well. A thorough treatment of this problem presents an attractive and challenging theoretical opportunity.

It is reasonable to ask at this point whether there are any experimental consequences of the excitonic scenario which are relatively model independent, and can therefore be firmly stated in advance of more accurate results? For this, we look to the discussion of Sec. V A focusing particularly on the properties in the undoped material. The excitonic scenario postulates symmetry breaking even without doping, which distinguishes it from, e.g., low-density ferromagnetism *a la* Wigner. All calculations so far appear to favor triplet ordering, which implies first a *constant (temperature independent at low T) susceptibility* in the insulator. Second, triplet ordering necessarily gives rise to *either* static spin moments or static spin currents (or both) within the unit cell. Because the latter are presumably difficult to observe, this is a less strong condition. Third, because the triplet state breaks spin-rotational invariance, it implies the existence of two low-energy collective ''magnon'' modes (presumably dispersing as $\omega \approx v_s|k|$ at low energies), which could be observable via inelastic neutron or Raman scattering. Fourth, an excitonic explanation for ferromagnetism upon doping requires that the ''pseudo-spin flip'' phenomena occur, and hence (in this sense) approximate SU(4) symmetry. This approximate symmetry implies the existence of additional collective modes with small excitation gaps.

It is natural to ask, given the above emphasis on the undoped state, whether the excitonic ferromagnet is itself truly a distinct phase of matter separate from the more familiar (theoretically) Wigner ferromagnet? The answer depends upon the extent to and manner in which the dopant *ions* influence the behavior of the electrons. In the models investigated to date, the dopants influence the material only insofar as to donate extra charge carriers, providing no perturbation to the *potential* felt by the electrons except to slightly increase the neutralizing positive background charge. In this treatment, the lattice point-group symmetries are strictly

maintained, and the excitonic ferromagnet is indeed a distinct state of matter: it exhibits more broken (point group) symmetries than the Wigner ferromagnet. In reality, the dopant ions most likely distribute randomly throughout the crystal, and thereby perturb the potential experienced by the electrons. This random potential explicitly breaks the lattice invariances, and washes out this sharp distinction between the excitonic and Wigner ferromagnets.

Whether this effect is of practical importance is unclear. The large *increase* of conductivity upon doping suggests that the electrons are not strongly scattered by the dopant ions. In any case, the physics at a low electron density is quite subtle. In particular, the environment around a nearly isolated dopant atom retains a large fraction of the symmetries of the pure lattice (e.g., a lanthanum dopant replacing strontium preserves cubic point-group symmetries around the lanthanum ion). Because electrons interact with only one impurity at a time at low densities, the symmetry of the local environment is expected to improve the distinction between Wigner and excitonic ferromagnets.

Clearly, further predictions are possible within more specific models. Several authors[6,7] recently pointed out the likelihood of phase separation at low electron densities. This occurs naturally in the pseudo-spin-flip picture, but because it has already been discussed, we will not dwell on it here. Probably most importantly, any excitonically ordered state by definition breaks the point-group symmetry of the lattice. This symmetry breaking is directly observable, but unfortunately depends in detail on the way it occurs. In particular, many of the triplet states that appear to be favored have less obvious order parameters, so that more work needs to be done to ascertain the appropriate experimental probes. Further modeling using the strong coupling approach promises to help resolve these and other issues.

ACKNOWLEDGMENTS

Thanks to C. M. Varma for stimulating interest in this problem, and to Z. Fisk for providing copies of experimental data. This research was supported by the NSF CAREER program under Grant No. NSF-DMR-9985255.

[1] D. P. Young *et al.*, Nature (London) **397**, 412 (1999).
[2] L. V. Keldysh and Yu. V. Kopaev, Fiz. Tverd. Tela (Leningrad) **6**, 2791 (1964) [Sov. Phys. Solid State **6**, 2219 (1965)].
[3] B. I. Halperin and T. M. Rice, in *Solid State Physics*, edited by F. Seitz, D. Turnbull, and H. Ehrenreich (Academic Press, New York, 1968), Vol. 21.
[4] B. A. Volkov *et al.*, Zh. Éksp. Teor. Fiz. **68**, 1899 (1975) [Sov. Phys. JETP **41**, 952 (1976)]; **70**, 1130 (1976) **43**, 589 (1976).
[5] M. E. Zhitomirsky, T. M. Rice, and V. I. Anisimov, Nature (London) **402**, 251 (1999).
[6] L. Balents and C. M. Varma, Phys. Rev. Lett. (to be published); cond-mat/9906259 (unpublished).
[7] V. Barzykin and L. P. Gor'kov, cond-mat/9906401 (unpublished).
[8] P. Fulde and R. A. Ferrell, Phys. Rev. A **135**, A550 (1964).
[9] A. I. Larkin and Yu. N. Ovchinnikov, Sov. Phys. JETP **20**, 762 (1965).
[10] Z. Fisk (private communication).
[11] S. Massidda *et al.*, Z. Phys. B: Condens. Matter **102**, 83 (1997); A. Hasegawa and A. Yanase, J. Phys. C **12**, 5431 (1979).
[12] E. Fradkin, *Field Theories of Condensed Matter Systems* (Addison-Wesley, Redwood City, CA, 1991).
[13] This mechanism is very much analogous to Zhang's SO(5) pseudo-spin-flip picture for high-temperature superconductivity. See S.-C. Zhang, Science **275**, 1089 (1997).
[14] Y. Nagaoka, Phys. Rev. **147**, 392 (1966).
[15] M. Veillette and L. Balents (unpublished).
[16] An alternative large N analysis, which might be expected to be *quantitatively* accurate for such an SU(4)-invariant model, is currently under investigation.
[17] H. Matsuda and T. Tsuneto, Suppl. Prog. Theor. Phys. **46**, 411 (1970); K. Liu and M. Fisher, J. Low Temp. Phys. **10**, 655 (1973).
[18] This is the second qualitative difference to emerge from the strong-coupling limit relative to weak coupling, where a singlet-triplet coexistence is preferred (Ref. 6).